Accepted Manuscript

Inhibition of LDL oxidation and inflammasome assembly by nitroaliphatic derivatives. Potential use as anti-inflammatory and anti-atherogenic agents

Nicolás Cataldo, Bruno Musetti, Laura Celano, Claudio Carabio, Adriana Cassina, Hugo Cerecetto, Mercedes González, Leonor Thomson

PII: S0223-5234(18)30840-7

DOI: 10.1016/j.ejmech.2018.09.062

Reference: EJMECH 10773

To appear in: *European Journal of Medicinal Chemistry*

Received Date: 4 July 2018

Revised Date: 4 September 2018

Accepted Date: 25 September 2018

Please cite this article as: Nicolá. Cataldo, B. Musetti, L. Celano, C. Carabio, A. Cassina, H. Cerecetto, M. González, L. Thomson, Inhibition of LDL oxidation and inflammasome assembly by nitroaliphatic derivatives. Potential use as anti-inflammatory and anti-atherogenic agents, *European Journal of Medicinal Chemistry* (2018), doi: https://doi.org/10.1016/j.ejmech.2018.09.062.

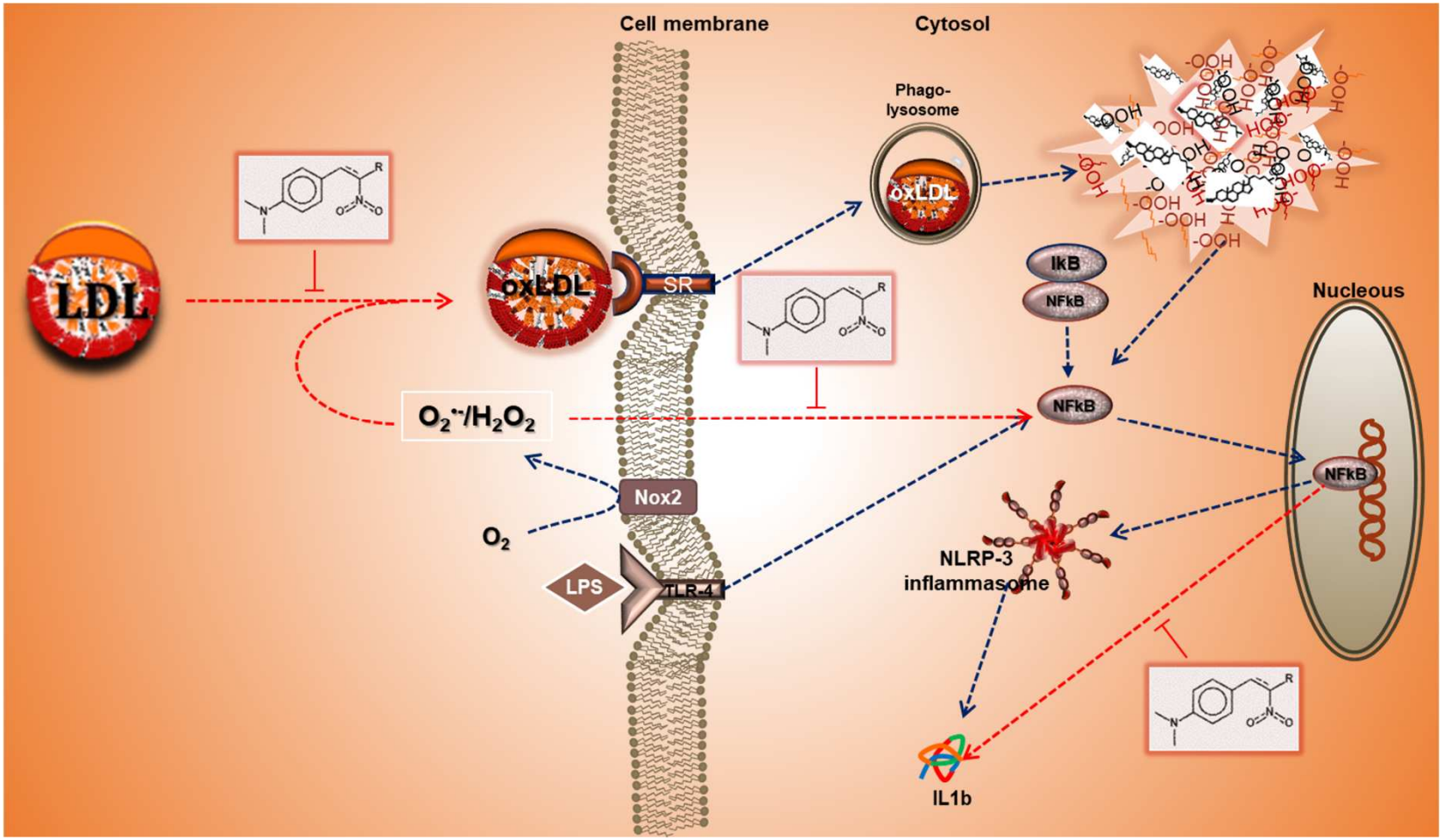
Cell membrane
Cytosol
Phago-
lysosome
LDL
oxLDL
SR
oxLDL
IkB
NFkB
Nucleous
$O_2^{\bullet-}/H_2O_2$
NFkB
Nox2
NFkB
O_2
NLRP-3
inflammasome
LPS
TLR-4
IL1b

Inhibition of LDL oxidation and inflammasome assembly by nitroaliphatic derivatives. Potential use as anti-inflammatory and anti-atherogenic agents

Nicolás Cataldo[a,b,*], Bruno Musetti[a,b,*], Laura Celano[a,1], Claudio Carabio[a], Adriana Cassina[c,d], Hugo Cerecetto[b], Mercedes González[b†], Leonor Thomson[a,c**]

[a]Laboratorio de Enzimología, Instituto de Química Biológica, Facultad de Ciencias, Universidad de la República. Iguá 4225, Montevideo, 11400, Uruguay.
[b]Grupo de Química Medicinal, Laboratorio de Química Orgánica, Facultad de Ciencias, Universidad de la República, Iguá 4225, Montevideo, 11400, Uruguay
[c]Center for Free Radical and Biomedical Research, Facultad de Medicina, Universidad de la República, General Flores 2125, Montevideo, 11800, Uruguay.
[d]Departamento de Bioquímica, Facultad de Medicina, Universidad de la República. General Flores 2125, Montevideo, 11800, Uruguay.

[†]Professor Mercedes Gonzalez passed away on May 21,2018.
*Both authors contributed equally to this work.
**Corresponding author: L. Thomson Facultad de Ciencias, Universidad de la República, Iguá 4225, 11400, Montevideo, Uruguay. Phone: 598-25258618 ext. 7214. E-mails: lthomson@fcien.edu.uy.

Abbreviations: oxLDL, oxidized low-density lipoprotein; LDL, low density lipoprotein; ORAC: oxygen radical absorbance capacity assay; AAPH, 2,2'-azo-bis (2-amidinopropane) dihydrochloride; DMSO, dimethyl sulfoxide; LPS, lipopolysaccharide (endotoxin) of the outer membrane of Gram-negative bacteria, INF-γ, interferon gamma.

[1] Present Address: Bioquímica y Microbiología General, Universidad Tecnológica (UTEC), Cno. Alejandro Malcom s/n, La Paz, Colonia, 70200, Uruguay.

ABSTRACT

We have previously shown the antioxidant and anti-inflammatory properties of several *para*-substituted arylnitroalkenes. Since oxidative stress and inflammation are key processes that drive the initiation and progression of atherosclerosis, in the present work the antioxidant, anti-inflammatory and anti-atherogenic properties of an extended library of aryl-nitroaliphatic derivatives, including several newly designed nitroalkanes, was explored. The antioxidant capacity of the nitroaliphatic compounds, measured using the oxygen radical absorbance capacity assay (ORAC) showed that the *p*-methylthiophenyl-derivatives were about three times more effective than Trolox to prevent fluorescein oxidation, independently of the presence or the absence of the double bond next to the nitro group. The peroxyl radical scavenger capacity of the *p*-dimethylaminophenyl-derivatives was even higher, being the reduced form of these compounds even more active. In fact, while the antioxidant capacity of 1-dimethylamino-4-(2-nitro-1Z-ethenyl)benzene and 1-dimethylamino-4-(2-nitro-1Z-propenyl)benzene was 4.2 ± 0.1 and 5.4 ± 0.1 Trolox Eq/mol, respectively; ORAC values obtained with the ethyl and the propyl derivatives were 10 ± 1 and 13 ± 2 Trolox Eq/mol, respectively. The *p*-dimethylamino-derivatives, especially the nitroalkanes, were also able to prevent LDL oxidation mediated by peroxyl radicals. Oxygen consumption due to the oxidation of fatty acids was delayed in the presence of the dimethylamino substituted compounds, only the alkanes interrupted the chain of lipid oxidations decreasing the rate of oxygen consumption. Although the formation of foam cells in the presence of oxidized-LDL (oxLDL) remained unaffected, the molecules containing the dimethylamino moiety were able to decrease the expression of IL-1β in LPS/INF-γ challenged macrophages.

Key words: arylnitroalkanes, atherosclerosis, antioxidants, anti-inflammatory

INTRODUCTION

Since cardiovascular and neurological complications of atherosclerosis are the main causes of morbidity and mortality worldwide [1], and because the attempt to improve cardiovascular outcomes have been unsuccessful, there is an urgent need of new therapies to increase life expectancy and improve the quality of life of atherosclerotic patients. Lowering cholesterol excess, restoring normal levels of blood pressure and commitment to a heart healthy lifestyle are key strategies to prevent major cardiac events, however intervention in additional mechanisms like vascular inflammation and oxidative stress are also important therapeutic targets in atherosclerosis [2]. For example, the activation of inflammasomes, in particular the nucleotide-binding oligomerization domain (NOD)-like receptor containing pyrin domain 3 (NLRP3) inflammasome, is now emerging as a critical molecular mechanism for many degenerative diseases, including atherosclerosis [3,4]. A plethora of danger signals are able to trigger the assembly of the NLRP3 inflammasome, including molecular patterns derived from pathogens (PAMPs), including lipopolysaccharides of the outer membrane of bacteria (like LPS), but also modified endogenous molecules with the so called danger associated molecular patterns (DAMPs) [5].

Oxidation and nitration of proteins and lipids generate neo-epitopes which are recognized as DAMPs by specific cell receptors [6–8]. In fact, oxidized LDL (oxLDL) is recognized by TLR4/6 and scavenger receptors triggering inflammatory cascades. Phagocytosis of the modified lipoprotein will ultimately transform subendothelial macrophages in lipid-laden foam cells [9,10]. Uncontrolled accumulation of cholesterol crystals, from LDL, damages the lysosomal membrane causing the leakage of peptidases into the cytosol and the hydrolytic activation of caspase 1 [11–14]. Simultaneously, NFκB dependent pathways cause the expression and assembly of the NLRP3 inflammasome with the subsequent activation of caspase 1. Caspase 1 is the hydrolytic enzyme responsible for activating IL-1β, an important mediator of the inflammatory response [15–17]. Although several intents were done to decrease the inflammatory response by the use of non-steroidal anti-inflammatory and biological agents, disappointing results were found during phase III trials [18,19].

In a previous report we developed a series of simple arylnitroalkene derivatives

with different stereoelectronic properties, able to release •NO and to scavenge the highly reactive products of peroxynitrite decomposition, •OH and $•NO_2$ [20]. Our lead compounds, especially 1-dimethylamino-4-(2-nitro-1*Z*-ethenyl)benzene (**1**) and 1-dimethylamino-4-(2-nitro-1*Z*-propenyl)benzene (**2**), and to a lesser extent 5-(2-nitro-1*Z*-propenyl)benzo[*d*][1,3]dioxol (**4)** (Figure 1A), also shown significant analgesic, anti-inflammatory, and anti-arthritic properties in animal models [21]. The pharmacologic effects were as least in part mediated by inhibition of prostaglandin H synthase, but the compounds were also able to prevent the activation of the matrix metallopeptidase 9 (MMP-9) [21]. Since IL-1β has been shown to induce MMP-9 production through activation of p42/p44 MAPK, p38 MAPK, JNK, and NF-κB pathways [22], the anti-inflammatory properties of the nitroalkene derivatives could also be due to interference in one or more steps related to or triggered by the assembly of the inflammasome, and in consequence could be suitable for the protection of the cardiovascular system as a multitarget therapy, by preventing LDL oxidation and also ameliorating inflammation. To test this hypothesis and with the interest of knowing more about the relationship between the structure and bioactivity, the capacity of twenty aryl-nitroaliphatic compounds to react with peroxyl radicals preventing LDL oxidation and ameliorate the production of IL-1β by LPS/INF-γ challenged macrophages was analyzed.

Since in our previous studies [20,21] we found that the presence of electron donor moieties at the phenyl group play relevant roles for the bioactivity, we designed new *p*-substituted-phenyl derivatives with similar electronic properties (Figure 1B). On the other hand, to explore the relevance of the double bond next to the nitro group in the nitroalkene moiety and since little is known about the bioactivity of nitroalkanes, we designed and tested several reduced derivatives (Figure 1B).

A)

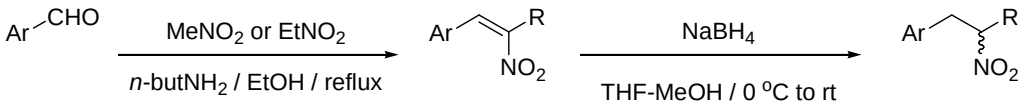

1, -R= -H, -Ar= -Ph-4-(NMe_2)
2, -R= -Me, -Ar= -Ph-4-(NMe_2)
3, -R= -H, -Ar= -Ph-3,4-(-OCH_2O-)
4, -R= -Me, -Ar= -Ph-3,4-(-OCH_2O-)
5, -R= -H, -Ar= -Ph-4-OMe
6, -R= -Me, -Ar= -Ph-4-OMe
7, -R= -H, -Ar= -Ph-4-SMe
8, -R= -H, -Ar= -Ph-4-(NHAc)
9, -R= -H, -Ar= -2-thienyl
10, -R= -Me, -Ar= -2-thienyl
11, -R= -H, -Ar= -Ph
12, -R= -Me, -Ar= -Ph
13, -R= -H, -Ar= -Ph-4-Cl
14, -R= -Me, -Ar= -Ph-4-Cl
15, -R= -H, -Ar= -Ph-4-Br
16, -R= -Me, -Ar= -Ph4-Br

17, -R= -H, -Ar= -Ph-4-(NMe_2)
18, -R= -Me, -Ar= -Ph-4-(NMe_2)
19, -R= -H, -Ar= -Ph-4-SMe
20, -R= -H, -Ar= =Ph-4-(NHAc)

B)

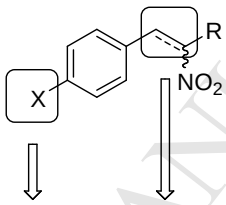

structural modifications proposed herein

Figure 1. Studied derivatives. A. Synthetic procedures for nitroalkenes (obtained as *Z*-isomers) and nitroalkanes. **B**. Design of new compounds.

RESULTS

1. Synthesis

The synthesis of the already reported library of arylnitroalkenes was performed via Henry reaction as described [20,21]. In addition two new unsaturated derivatives 1-methylthio-4-(2-nitro-1*Z*-ethenyl)benzene (**7**) and the 1-acetylamino-4-(2-nitro-1Z-ethenyl)benzene (**8**) were generated (Figure 1A). The synthesis of the reduced compounds, 1-dimethylamino-4-(2-nitroethyl)benzene (**17**), 1-dimethylamino-4-(2-nitropropenyl)benzene (**18**), 1-methylthio-4-(2-nitroethyl)benzene (**19**) and 1-acetylamino-4-(2-nitroethyl)benzene (**20**), was performed by mild reduction of the double bond from the appropriate nitroalkene (**1**, **2**, **7** and **8**, respectively) using sodium borohydride. Methanol was used as co-solvent, since the methoxylation of borohydride favors the selective alkene-reduction leaving the nitro group unchanged [23,24]. Derivatives **17-20** (Figure 1A) were obtained in good to very good yields (61-

86 %) after chromatographic purifications. The new products were structurally characterized by ^{1}H NMR and ^{13}C spectroscopy, and their purity established by TLC and elemental microanalysis (C, H, N, S) (Table S1). In the ^{1}H NMR spectra, the presence of the nitroalkanes of interest, **17-20** (Figure 1A), was evidenced by the appearance of two triplets or triplets of doublets at high field (δ ~4.8 and ~3.2 ppm) due to the loss of the unsaturation, provoking that the methylene protons became flanked by two neighboring protons each and the consequent disappearance of the characteristic nitroalkene-olefinic protons at low field (δ ~7.7 and ~7.5 ppm), (see examples in Figure S1). For nitroalkane **19** the diastereotopic properties of the methylene protons belonging to the nitroethyl-moiety (triplets of doublets) were clearly observed in the ^{1}H NMR spectrum (Figure S1)). The study of the proton-carbon correlations was carried out through HSQC and HMBC experiments. The *Z*-isomeric form of the new nitroalkenes, **7** and **8**, was confirmed using the coupling constants H-H for the alkene-systems and by NOE-diff experiments.

2. Reaction with peroxyl radicals

In view of the already reported results on the reaction of aryl nitroalkenes with biologically generated oxidants [20,21] we decided to explore the reactivity of these kind of derivatives with peroxyl radicals using an standard technique, the oxygen radical absorbance capacity (ORAC). This technique measures the loss of auto-fluorescence of fluorescein after oxidation by the products of the thermal decomposition of 2,2'-azobis(2-amidinopropane) dihydrochloride (AAPH). The main degradation pathways of AAPH in aqueous solutions, hydrolysis (Eq. 1) and thermal decomposition (Eq. 2), generate unstable carbon centered radicals (R$^{\bullet}$) [25].

$$\mathrm{AAPH} + \mathrm{HO}^{-} \xrightarrow{1.3x10^{-5}s^{-1}} \mathrm{R}_1^{\bullet} + \mathrm{R}_2^{\bullet} \quad (1)$$

$$\mathrm{AAPH} \xrightarrow{2.1\mathrm{x}10^{-6}\mathrm{s}^{-1}} \mathrm{N}_2 + 2\mathrm{R}_1^{\bullet} \quad (2)$$

The radicals react at almost diffusion-controlled rate with molecular oxygen to yield peroxyl radical (R–OO$^{\bullet}$) (Eq. 3), which decomposes mainly to alkoxyl radicals (Eq. 4).

$$2\mathrm{R}^{\bullet} + 2\mathrm{O}_2 \rightarrow 2\mathrm{ROO}^{\bullet} \quad (3)$$

$$2\mathrm{ROO}^{\bullet} \rightarrow 2\mathrm{RO}^{\bullet} + \mathrm{O}_2 \quad (4)$$

Both, peroxyl and alkoxyl radicals react fast with reduced targets (XH) (Eq. 5).

$$\mathrm{ROO}^{\bullet}(\mathrm{RO}^{\bullet}) + \mathrm{XH} \rightarrow \mathrm{ROOH}(\mathrm{ROH}) + \mathrm{X}^{\bullet} \quad (5)$$

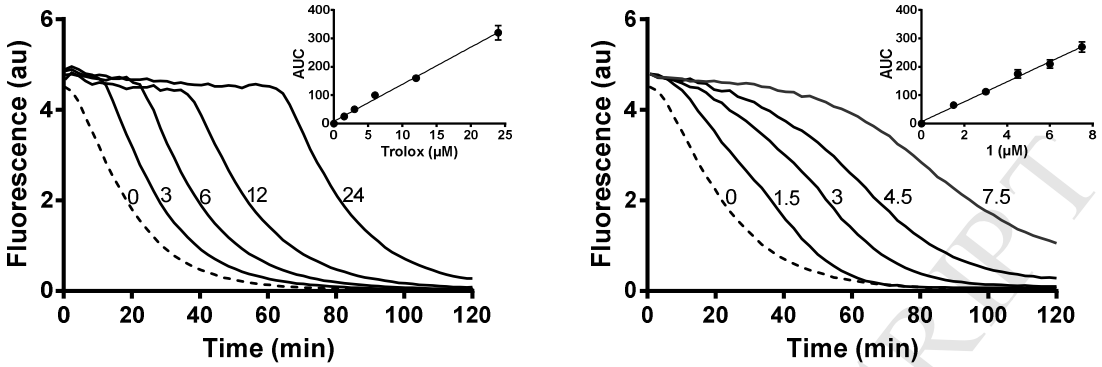

Figure 2. Oxygen radical antioxidant capacity. Representative time courses of fluorescein (7.5 nM) oxidation by AAPH (30 mM) at 37 ℃ in 75 mM phosphate buffer pH 7.4, 100 µM DTPA, in the presence of Trolox (3-24 µM) (**A**) and **1** (1.5-7.5 µM) (**B**) at λexc 485 nm and λem 512 nm. Fluorescein oxidation in the absence of antioxidants was represented by dashed lines. Numbers above lines denote antioxidant concentration (µM). Insets show linear fit of the areas under the curves (AUC) as a function of antioxidant concentration. AUC values are expressed as media ± SD of three independent determinations.

The capacity of the selected compounds to trap both radicals preventing fluorescein oxidation was compared against the same property of 6-hydroxy-2,5,7,8-tetramethylchroman-2-carboxylic acid (Trolox), a hydrosoluble analogous of vitamin E used as standard (Figure 2). The dimethylamino derivatives, **1**, **2**, **17** and **18**, were the most potent antioxidants (Table 1), confirming our previous results for the nitroalkenes (**1** and **2**) and showing a potential higher antioxidant capacity for both saturated analogous (nitroalkanes **17** and **18**) [20,21]. In fact, the capacity to trap peroxyl radicals by compounds **1** and **2** was more than 4 times higher than the capacity of Trolox, but surprisingly, the reduction of the double bond on the side chain of both dimethylamino derivatives to generate compounds **17** and **18**, increased significantly the antioxidant capacity of the products. Actually, **18** was 10 times more effective than Trolox to prevent the loss of fluorescence while the antioxidant capacity of **17** was even higher (Table 1).

Table.1. ORAC values of the analyzed compounds.

EF[a]	Derivative	TEq[b,c]	Derivative	TEq[b,c]
med[d]	**1**	**4.2 ± 0.1**	**17**	**13 ± 2**
	2	**5.4 ± 0.1**	**18**	**10 ± 1**
	3	0.72 ± 0.01		
	4	**1.6 ± 0.2**		
	5	0.46 ± 0.03		
	6	0.46 ± 0.02		
	7	**3.5 ± 0.3**	**19**	**2.8 ± 0.2**
	8	0.63 ± 0.07	**20**	0.26 ± 0.06
	9[e]	0.43 ± 0.07		
	10[e]	0.54 ± 0.01		
we[f]	**11**	0.29 ± 0.01		
	12	0.37 ± 0.06		
med-iew[g]	**13**	0.44 ± 0.01		
	14	0.39 ± 0.02		
	15	0.44 ± 0.04		
	16	0.45 ± 0.06		

[a] EF: electronic effect of the aryl substituent.
[b] Trolox equivalents (TEq) were determined by ORAC as in Fig. 2.
[c] Results are the average of three independent experiments ± SD.
[d] med: electron-donor group by mesomeric effect.
[e] bioisosters of derivatives **11** and **12**, respectively.
[f] we: without electronic effect.
[g] med-iew: electron-donor group by mesomeric effect and electron-withdrawing group by inductive effect.

The antioxidant capacity of the derivatives bearing the 1,3-dioxol system was higher than the one observed with Trolox in the molecule bearing the nitropropenyl framework (**4**) and was slightly lower than 1 in the molecule with the nitroethenyl framework (**3**), the differences between both compounds was in concordance with our previous reports [20,21]. While the compounds carrying other substituents, including the methoxy (**5**, **6**), hydrogen (**11**, **12**) and halide (**13**, **14**, **15**, and **16**) groups were ~50% less effective than Trolox, without any consistent difference attributable to the presence of the additional methyl group in R (Table 1). Additionally, we studied the antioxidant ability of derivatives **9** and **10** (Table 1), that hold a thiophene heterocycle instead of the phenyl group, potential bioisosters of derivatives **11** and **12**, respectively. Derivatives **9** and **10** displayed higher activity than **11** and **12,** probably as a result of the mesomeric-electron donor ability of the sulfur in the heterocycle.

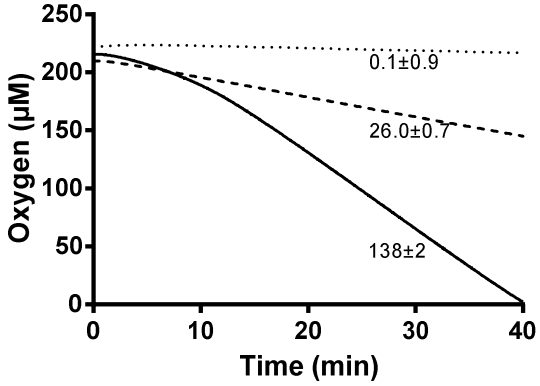

Figure 3. LDL oxidation by AAPH. Oxygen consumption by LDL (0.2 mg mL^{-1}) alone (dotted line), AAPH (30 mM) alone (dash line) and LDL (0.2 mg mL^{-1}) plus AAPH (30 mM) (continuous line) was analyzed at 37^{o} C in 75 mM phosphate buffer, pH 7.4, using a high-resolution oxygen electrode as described in Materials and Methods. Traces are representative of three independent determinations performed in the same condition using a different purification batch of LDL. Numbers below lines represent mean oxygen consumption (pmol O_2 ml^{-1} s^{-1} ± SD) (n = 3)

In addition, the capacity of the molecules to prevent fluorescein oxidation was preserved after substitution of the tertiary amine present in the nitroalkene **1** by a thioether moiety in the nitroalkene **7**, but it was significantly decreased in the presence of an acetamido group in the phenyl moiety in nitroalkene **8**, while the reduction of the double bond in both compounds to generate nitroalkanes **19** and **20**, respectively, failed to improve the antioxidant properties of the products. Clearly, electronic effects played relevant roles in the antioxidant profiles, thus derivatives with negative or near to zero Hammett σ_p and near to zero inductive σ_I constants, for *p*-substituents of the phenyl moiety, displayed the best profiles, i.e. σ_p = -0.83 and σ_I = 0.06 for –$N(Me)_2$; σ_p = 0.00 and σ_I = 0.23 for –SMe; σ_p = -0.15 and σ_I = 0.26 for –NAc; σ_p = -0.27 and σ_I = 0.27 for –OMe; and σ_p = 0.23 and σ_I = 0.47 for –Cl [26]

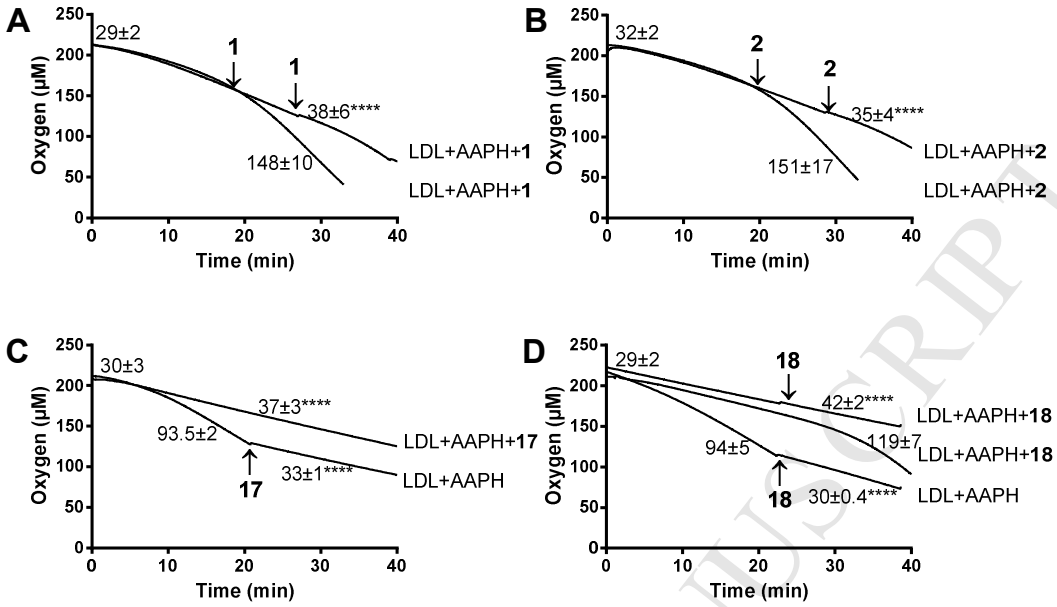

.

Figure 4. Effect of NA on the oxidation of LDL by AAPH. Representative traces of oxygen consumption by 0.2 mg mL^{-1} LDL plus 30 mM AAPH assayed in the absence (LDL+AAPH) and in the presence of 20 μM **1** (**A**), **2** (**B**), **17** (**C**) and **18** (**D**) as specified at the right of each trace, the arrows indicate the addition of the molecules during the course of the reaction. Numbers next to the lines depict the mean rate of oxygen consumption (pmol O_2 ml^{-1} s^{-1}) from three independent experiments ± SD. Statistically significant differences (****$p<0.0001$) were found between the rate of oxygen consumption by the system in the absence and the presence of the analyzed compounds.

3. Protection of LDL from peroxyl radical mediated oxidations.

Since several of the synthetic compounds, were able to effectively trap peroxyl and alkoxyl radicals derived from AAPH decomposition, and since these radicals can trigger lipid oxidation, the more effective compounds to prevent fluorescein oxidation were selected to explore the capacity to prevent LDL oxidation by AAPH measuring oxygen consumption. The rate of oxygen consumption by 30 mM AAPH at 37^o C (26.0 ± 0.7 pmol O_2 ml^{-1} s^{-1}) (Figure 3) was similar to the already reported decomposition rate [25]. After reaction with oxygen, AAPH-derived peroxyl and alkoxyl radicals (Eq. 3 and 4) can react with different biological molecules leading mainly to the production

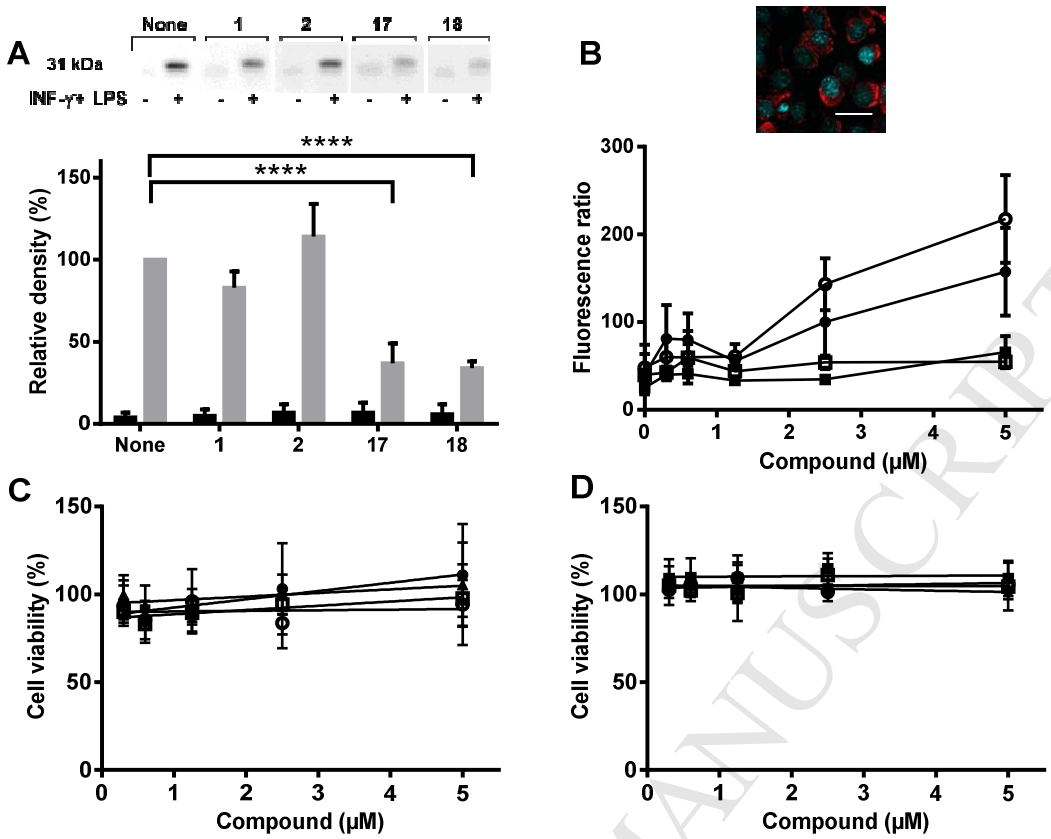

Figure 5. Effect on IL-1β expression and ox-LDL internalization by J774 cells. A. IL-1β expression by J774 cells incubated for 1 h in the absence (None) and the presence of **1**, **2**, **17** and **18** (5 μM), and challenged for 4 h with INF-γ (400 U mL^{-1}) and LPS (8 μg mL^{-1}) was analyzed. A representative western blot is shown on the top, while the densitometric analysis of IL-1β bands is shown on the bottom. Bars represent mean values of the protein bands from non-challenged cells (black bars) and the cells treated with INF-γ plus LPS (grey bars) from three independent experiments. (****, $p<0.0001$). **B**. A representative merged image showing J774 cells loaded with ox-LDL DiI (red) and the nucleus stained with Hoechst 3342 (blue) is shown on the top (Bar = 25 μm). The bottom graph represents the ratio between the fluorescence due to ox-LDL DiI (λexc 549, λem 565) and Hoechst (λexc 352, λem 461) against the concentration of **1** (●), **2** (○), **17** (■) and **18** (□). J774 cells were incubated in 96 well plates, in the presence of increasing concentrations (0.3-5 μM) of the compounds for 1 h and settled for 4 h with ox-LDL DiI and the fluorescence at both wavelengths was read using a plate reader. **C.** Confluent cell monolayers were incubated for 2 h in the presence of increasing concentrations (0.3-5 μM) of **1** (●), **2** (○), **17** (■) and **18** (□) and the effect on cell viability was measured by the MTT reduction assay. **D.** As in **C** but cell viability was measured after 24 h of incubation with the compounds.

of carbon centered radicals ($X^{\bullet}$) (Eq. 5). The reaction of $X^{\bullet}$ with molecular oxygen give rise to peroxyl radicals ($XOO^{\bullet}$) (Eq. 6). The reaction of peroxyl radicals with another reduced molecule starts a chain of radical mediated reactions, known as propagation phase (Eq. 7).

$$X^{\bullet} + O_2 \rightarrow XOO^{\bullet} \quad (6)$$

$$XOO^{\bullet} + XH \rightarrow XOOH + X^{\bullet} \quad (7)$$

Oxygen consumption by LDL in the presence of AAPH showed the characteristic biphasic profile of lipid oxidation, with an initial slow phase, due to the presence of endogenous antioxidants; followed by a propagation phase of fast oxygen consumption (Figure 3). In the first phase, the rate of oxygen consumption in the presence of LDL plus AAPH was similar to the rate with AAPH alone, consistent with the silent (regarding oxygen consumption) initial phase of lipid oxidation. Approximately 7 min later the entrance in the propagation phase triggered a burst of oxygen consumption with a rate of 138 ± 2 pmol O_2 ml^{-1} s^{-1} (Figure 3).

The addition of 20 μM of the selected compounds (**1**, **2**, **17**, and **18)** before AAPH delayed the transition from the initiation to the propagation phase (Figure 4). While the propagation phase in the presence of nitroalkenes **1** and **2** started ~20 min after the addition of AAPH, nitroalkanes **17** and **18** were even more effective protecting LDL form peroxyl radicals mediated oxidation. In fact, in the presence of **18** the initiation phase last ~30 min, while **17** delayed the beginning of the propagation phase in more than 40 min (Figure 4). The addition of the selected molecules during the reaction also delayed the entrance of the system into the propagation phase. The addition of successive boluses of 1 and 2 before the beginning of the propagation phase delayed its appearance, however both compounds were ineffective when added after the beginning of this phase (Figure S3). Conversely, **17** and **18** were also able to stop the oxidation process even if added after the beginning of the propagation phase, reversing the rate of oxygen consumption to a level close to that of AAPH alone (Figure 4C and D).

4. *In vitro* analysis of the anti-inflammatory and anti-atherogenic properties.

To explore the mechanisms involved in the anti-inflammatory properties of the dimethylamino substituted nitroalkenes already reported [20], **1** and **2**, the ability of these compounds, together with the reduced analogues described herein, **17** and **18**, to interfere with IL-1β activation was studied. Murine macrophages (J774 cells) were incubated for 4 hours in the presence of INF-γ plus LPS and the expression of IL-1β was explored by western blot. As expected, the expression of IL-1β increased significantly in cell cultures exposed to the INF-γ and LPS. The addition of the

dimethylamino derivatives decreased significantly the expression of the cytokine, being the saturated compounds more effective than the corresponding unsaturated ones (Figure 5A). Since neither LDL nor oxLDL were able to stimulate the synthesis of pro-IL-1β under our experimental conditions (Figure S3), and because the deposition of foam cells into the artery wall is one of the earliest steps in the progression of the atherosclerotic plaque [10], the capacity of the selected compounds to prevent the internalization of ox-LDL by murine macrophages was explored. The complex between oxLDL and the lipophilic fluorescent dye DiI was effectively taken up by J774 cells (Figure 5B), as described before [27]. The fluorescent signal appeared into the cells both in the absence and the presence of the compounds. Moreover, in the presence of the higher concentrations used (2.5-5 μM) of **1** and **2** a significant increase in the amount of fluorescence due to the labeled lipoprotein was observed, discarding any interference of the compounds with the phagocytic process. To rule out the possibility that the effect of the analyzed molecules on the expression of IL-1β were due to cellular dead, cell viability and function were analyzed by investigating the capacity of the cellular mitochondria to reduce the tetrazolium compound MTT. The cell survival remained unchanged after 2 and 24 h of incubation in the presence of the analyzed concentrations (0.3-5 μM) of both nitroalkenes and nitroalkanes, being the amount of formazan formed equivalent to the amount generated in the presence of vehicle alone (Figure 5C and D).

CONCLUSIONS

The main cardiovascular risk factors, including hypertension, smoking, physical inactivity, obesity, hyperlipemia, and diabetes mellitus are associated with inflammation and oxidative stress [28]. In animal models, vascular cell dysfunction, intimal hypertrophy, and the formation and destabilization of atherosclerotic plaques were associated with an increased oxidant status [29,30]. Therefore, oxidative stress was considered as a major contributor to the development of cardiovascular diseases and antioxidant treatments were proposed as promising therapeutic strategies. However, the attempts to improve cardiovascular outcomes by mean of antioxidant vitamin supplementation were unsuccessful, remaining the incidence of major cardiovascular events unchanged [31,32]. Moreover, the increase of the risk of lung cancer in smoker males after supplementation with β-carotene [22] discouraged the use of liposoluble vitamins and other unspecific antioxidants in primary care. Those findings have prompted the development of more specific antioxidants, able to leave the vascular redox balance intact, preserving the normal levels of $^{\bullet}NO$ and H_2O_2, since both have been shown as essential molecules in redox signaling. We have already reported the capacity of several *p*-phenylsubstituted nitroalkenes to scavenge oxygen and nitrogen derived oxidants [20]. In particular the dimethylamino derivatives were able to specifically react with the radicals derived from $ONOO^-$ homolysis, $^{\bullet}OH$ and $^{\bullet}NO_2$, without significant reaction with $^{\bullet}NO$ or H_2O_2 [20]. The same compounds also showed remarkable anti-inflammatory and analgesic properties due to inhibition of prostaglandin H synthase [21]. In consequence these compounds can be proposed as candidates for multitarget therapy to ameliorate the inflammatory process and the consequent oxidative stress.

To reinforce our previous findings [20,21], in the present work the potential anti-atherogenic properties of the molecules analyzed so far and several new derivatives was investigated. As observed before [20], the *p*-dimethylamino-substituted nitroalkenes (**1** and **2**) and the newly synthesized nitroalkanes (**17** and **18**) were highly effective antioxidants. In fact, the four compounds acted as peroxyl radical scavengers preventing the oxidation of fluorescein and LDL. In particular, nitroalkanes **17** and **18** acted as chain breaking antioxidants, decreasing the consumption of oxygen due to the propagation phase of LDL-lipid oxidation. Both the survival and the capacity of J774 cells to recognize and phagocyte oxLDL remined

unaffected in the presence of the tested compounds (**1**, **2**, **17** and **18**). However, the same compounds were able to interfere with one of the main products of inflammasome activation, the expression of IL-1β. In fact, the molecules decreased the expression of IL-1β induced by LPS and INF-γ, reinforcing the anti-inflammatory properties of the dimethylamino-derivatives, having the nitroalkanes even better antioxidant and anti-inflammatory properties than the original nitroalkenes.

Several biological agents with anti-inflammatory properties are being tested for the treatment of atherosclerosis [33]. Recently, the results of the CANTOS trial (Canakinumab Anti-Inflammatory Thrombosis Outcomes Study) showed that canakinumab, a monoclonal IL-1β–neutralizing antibody, reduced the risk of recurrent cardiovascular events in patients with prior heart attack [34,35]. However, treatments with biological agents are expensive and the risk of the long-term therapy is still unknown or has been proven to be largely disappointing due to an increase in the risk of opportunistic infections or cardiovascular complications [18,19]. Because of that, the search for new compounds able to decrease the inflammatory response associated with chronic diseases, as atherosclerosis, is a priority. In this context our compounds can become an effective and economic alternative to delay the progression of atherosclerosis and prevent the appearance of major cardiac events.

MATERIALS AND METHODS

Experimental

Materials were purchased from Sigma-Aldrich Co. (USA) and Across Organic (Janssen Pharmaceutical, Geel, Belgium). All solvents were dried and distillated with conventional methods prior to use, and the synthesis carried under nitrogen atmosphere. Compounds **1-6**, **9-16**, and **18** were prepared as previously described [20,24]. The synthesized compounds were chemically characterized by thin layer chromatography (TLC), nuclear magnetic resonance (NMR) and elemental microanalyses (CHN). Alugram SIL G/UV254 (Layer: 0.2 mm) (Macherey-Nagel GmbH & Co. KG., Düren, Germany) was used for TLC. The purity of compounds was determined by elemental microanalyses performed on a Carlo Erba Model EA1108 elemental analyzer from 48 h-vacuum-dried samples. The analytical results for C, H, N and S were within ± 0.4 of the theoretical values. The ^{1}H and ^{13}C NMR spectra were recorded on a Bruker DPX 400 (400 MHz), using TMS as the internal standard and with the indicated deuterated solvent; the chemical shifts are reported in ppm (δ) and coupling constants (J) values are given in Hertz (Hz). Signal multiplicities are represented by: s (singlet), d (doublet) and td (triplet of doublet). NOE diff experiments were performed to establish the stereochemistry around the double bond.

General procedure for synthesis of nitroalkenes

In a rounded flask, a mixture of the corresponding aldehyde (0.8 mmol), anhydrous nitromethane (3 mL) and ammonium acetate (0.8 mmol) was stirred at 100 ^{o}C for 2 h. The solvent was evaporated *in vacuo* and the residue was treated with water (30 mL) and extracted with ethyl acetate (3 × 20 mL). The organic layer was successively washed with water (2 × 50 mL), HCl (1M, 2 × 25 mL) and brine (2 × 20 mL), dried with anhydrous sodium sulfate and evaporated *in vacuo*. The obtained solid was washed with *n*-hexane to yield the corresponding product.

1-Methylthio-4-(2-nitro-1*Z*-ethenyl)benzene (7): Yellow solid. (0.11 g, 61%) ^{1}H-NMR ($CDCl_3$, 400 MHz) δ (ppm): 7.60 (d, 1H, J=12.00), 7.47 (d, 1H, J=12.00), 7.29 (d, 2H, J=8.00), 7.27 (m, 2H), 2.55 (s, 3H). ^{13}C-NMR ($CDCl_3$, 100 MHz) δ (ppm): 145.0, 138.6, 136.1, 129.0, 125.3, 14.0. (Found: C, 55.1; H, 4.8; N, 6.9; S, 16.3%. $C_9H_9NO_2S$ requires C, 55.4; H, 4.7; N, 7.2; S, 16.4%).

1-Acetylamino-4-(2-nitro-1*Z*-ethenyl)benzene (8): Yellow solid. (0.10g, 78%) ^{1}H-NMR ($CDCl_3$, 400 MHz) δ (ppm): 7.69 (d, 1H, J=12.00), 7.62 (d, 1H, J=12.00), 7.36 (d, 2H, J=8.00), 7.25 (d, 2H, J=8.00), 2.06 ppm (s, 3H). ^{13}C-NMR ($CDCl_3$, 100 MHz) δ (ppm): 168.9, 142.8, 138.8, 130.9, 124.4, 118.5, 39.5. (Found: C, 58.5; H, 4.5; N, 13.4%. $C_{10}H_{10}N_2O_3$ requires C, 58.3; H, 4.9; N, 13.6%).

General procedure for synthesis of nitroalkanes

In a 25 mL round-bottom flask the corresponding nitroalkene (0.5 mmol) was dissolved in THF (1.6 mL) and MeOH (0.2 mL). After cooling at 0 ^{o}C, $NaBH_4$ (2.5 mmol) was added in four fractions and allowed to react for 40 min at room temperature under stirring. Then the solvent was distilled *in vacuo*, and the residue was treated with brine (10 mL) and extracted with ethyl ether (3 × 5 mL). The organic layer was dried with anhydrous sodium sulfate and the solvent was evaporated *in vacuo*. The compounds were purified by column chromatography (SiO_2, gradient of *n*-hexane:ethyl acetate).

1-Dimethylamino-4-(2-nitroethyl)benzene (17): Yellow solid (0.03 g, 86%). ^{1}H-NMR ($CDCl_3$, 400 MHz) δ(ppm): 7.08 (d, 2H, J=8.00), 6.70 (d, 2H, J=8.00), 4.56 (t, 2H, J=8.00), 3.24 (t, 2H, J=8.00), 2.94 (s, 6H). ^{13}C-NMR ($CDCl_3$, 100 MHz) δ (ppm): 149.8, 129.0, 122.5, 112.2, 76.5, 40.3, 32.3. (Found: C, 61.6; H, 7.4; N, 14.0%. $C_{10}H_{14}N_2O_2$ requires C, 61.8; H, 7.3; N, 14.4%).

1-Methylthio-4-(2-nitroethyl)benzene (19): Yellow oil (0.03 g, 86%). ^{1}H-NMR ($CDCl_3$, 400 MHz) δ(ppm): 7.23 (d, 2H, J=8.00), 7.08 (d, 2H, J=8.00), 4.95 (td, 1H, J=8.00, J=12.00), 4.80 (td, 1H, J=8.00, J=12.00), 3.19 (td, 1H, J=8.00, J=12.00), 3.08 (td, 1H, J=8.00, J=12.00), 2.50 (s, 3H). ^{13}C-NMR ($CDCl_3$, 100 MHz) δ (ppm): 140.0, 130.2, 128.8, 126.8, 77.0, 32.0, 14.1. (Found: C, 54.5; H, 5.6; N, 6.9; S, 16.0%. $C_9H_{11}NO_2S$ requires C, 54.8; H, 5.6; N, 7.1; S, 16.3%).

1-Acetylamino-4-(2-nitroethyl)benzene (20): Yellow solid (0.03 g, 78%). ^{1}H-NMR (DMSO-d_6, 400 MHz) δ(ppm): 7.48 (d, 2H, J=8.00), 7.18 (d, 2H, J=8.00), 4.60 (t, 2H, J=8.00), 3.30 (t, 2H, J=8.00), 2.18 (s, 3H). ^{13}C-NMR (DMSO-d_6, 100 MHz) δ (ppm): 168.3, 137.5, 131.0, 129.4, 120.0, 76.0, 32.3, 24.6. (Found: C, 57.5; H, 5.6; N, 13.8%. $C_{10}H_{12}N_2O_3$ requires C, 57.7; H, 5.8; N, 13.5%).

Preparation of stock solutions. Stock solutions were prepared fresh in DMSO. Dilutions were made in phosphate buffer at pH and ionic strength according to each

experiment and corresponding. Controls of interference of DMSO and auto-fluorescence of the compounds were performed.

Evaluation of the antioxidant capacity of the compounds. The antioxidant capacity of the molecules was evaluated using the oxygen radical absorbance capacity (ORAC) method [36]. The decay of the fluorescence at λexc 485 nm and λem 512 nm due to oxidation of fluorescein (7.5 nM) by peroxyl radicals was followed during 140 min in a Varioskan Flash plate reader (Thermo Electron Corp., Finland) in 75 mM phosphate buffer, pH 7.4, with 100 μM DTPA at 37^{o} C. Peroxyl radicals were generated by thermal decomposition of 30 mM 2,2'-Azobis(2-amidinopropane) dihydrochloride (AAPH). As standard antioxidant, 6-hydroxy-2,5,7,8-tetramethylchroman-2-carboxylic acid (Trolox, 1.5-24 μM) was used. For the analysis, the curves of fluorescence vs time in the absence and in the presence of the compounds (1.3-13 μM) were normalized by dividing the values by the fluorescence at the beginning (f_0)., and the area under the curves (AUC) were then calculated using Ec. 9.

$$AUC = 1 + \sum_{i=1}^{i=140} \frac{f_i}{f_0} \quad (9)$$

Were f_i represents the fluorescence reading at time *i*. The net value was obtained by subtracting the AUC obtained in the absence (AAPH alone) from the area in the presence of antioxidant. The slope of a linear regression of AUC vs concentration was used to determine Trolox equivalents for each compound, as follows (Ec. 10):

$$Trolox\ Eq = \frac{Slope\ compound}{Slope\ Trolox} \quad (10)$$

Isolation of LDL from human plasma. Human plasma was obtained from blood voluntarily donated at the Hematology Department at Hospital de Clínicas. The procedures were in accordance with the Helsinki's Declaration and approved by the Institutional Committee. Each blood donor was informed of their right to refuse, the relevance of the investigation and the privacy (identity protection) of the information taken, an informed consent form was signed by each donor. Total blood (450 mL) was collected in primary bags containing 63 mL of anticoagulant solution CPD (129 mM dextrose, 105 mM citrate and 16 mM phosphate, Terumo Corporation, Tokyo, Japan) as described [37]. Blood bags were centrifuged using a Roto Silenta 63RS transfusion bag centrifuge (Hettich, Germany) at 2,200 rpm at 20 ^{o}C, plasma was transferred to a satellite bag and saved at -20 ^{o}C until use (maximum two weeks). The low-density lipoprotein (LDL) fraction was isolated from human plasma using a

density gradient performed by adding 0.28 g KBr per mL of plasma. Then NaCl 0.15 M was added on top and ultracentrifugation was performed at 300.000 g for 90 minutes at 4 ºC. The orange band, LDL fraction, was collected and dialyzed against phosphate buffered saline (PBS) prepared with 137 mM NaCl, 2.7 mM KCl, 10 mM Na_2HPO_4, 1.8 mM KH_2PO_4, pH 7.4. Protein concentration was evaluated at 280 nm (ε = 1 cm^{-1} $(mg/mL)^{-1}$).

LDL oxidation by AAPH. The capacity of the compounds to inhibit LDL oxidation by AAPH was measured as the rate of oxygen consumption using an Oxygraph 2 K (Oroboros Instruments Corp). Oxygen consumption by 0.2 mg/mL LDL and 30 mM AAPH, in the presence and the absence of the compounds (20 µM) was recorded at 37℃ under continuous stirring in 75 mM phosphate buffer, pH 7.4. The rate of oxygen consumption was calculated by means of the equipment software (DataLab) and expressed as pmol O_2 s^{-1}. mL^{-1}.

Fluorescent labeling and oxidation of LDL. The LDL fraction was labeled with the lipophilic fluorescent probe (2*Z*)-2-[(*E*)-3-(3,3-dimethyl-1-octadecylindol-1-yl-2-yl)prop-2-enylidene]-3,3-dimethyl-1-octadecylindole (DiI, AnaSpec, Fermont, CA) and subsequently oxidized as described before [27]. Briefly, the LDL fraction isolated as described before was bubble with nitrogen to remove oxygen and incubated in the presence of 50 µL of DiI (3 mg/mL in DMSO) per mg of LDL protein overnight in the dark at 37 ℃. Next day the solution of DiI-LDL (0. 1 mg/mL) was incubated with 5 µM $CuSO_4$ at 37 ℃ for 24 h, protected from light. Then the DiI-oxLDL complex was centrifuged at 30,000 g for 5 h at 4 ℃. The band distributed in the middle layer containing DiI-oxLDL was isolated and dialyzed against PBS with 0.24 mM EDTA. The protein content was determined by the bicinchoninic acid technique (Sigma-Aldrich). Samples were sterilized by filtration and stored at 4 ℃, in the dark for a maximum of 3 weeks.

Macrophage J774 culture. The murine macrophage-like cell line J774 (ATCC- TIB-67, American Type Culture Collection) was maintained by passage in Dulbecco's Modified Eagle Medium (DMEM) (Gibco, Invitrogen) containing glutamine (4 mM), sodium pyruvate (110 mg L^{-1}), glucose (4.5 g L^{-1}), penicillin (100 U mL^{-1}), streptomycin (100 mg L^{-1}), and 10 % heat-inactivated fetal bovine serum (FBS). The cells were plated and incubated at 37 ºC in 5 % CO_2 and 95 % air atmosphere.

Foam cell formation. Following already published procedures [27,38]**,** J774 cells at ~80% confluence in 24 well plates (~2×10^5 cel/well) were incubated in the absence and the presence of 5 µM of the analyzed compounds in DMEM for 1 h, after that DiI-oxLDL (10 µg/mL) was added to the wells and the cells were incubated for 4 hours at 37 ^{o}C and 5% CO_2. Subsequently, the cells were washed three times with PBS with 2 mg/mL BSA and twice with PBS. To stain the nuclei, the cells were incubated for 10 minutes with 10 µg/mL Hoechst 3342 (AnaSpec, Fermont, CA) and washed three times with PBS. Cellular uptake of DiI-oxLDL was observed using a Zoe Fluorescent Cell Imager (Bio-Rad Laboratories Inc., Hercules, CA) using a red filter for DiI and a blue one for Hoechst. Alternatively, the cell culture was done in 24 well plates and the cells treated in the same way, and quantifications performed using a Varioskan Flash plate reader (Thermo Electron Corp., Finland) as described in [39]. Results were expressed as the ratio between the fluorescence emitted by DiI (λ_{Exc} = 549 nm, λ_{Em} = 565 nm) and the fluorescence emitted by Hoechst (λ_{Exc} = 352 nm, λ_{Em} = 461 nm).

Cytotoxicity analysis. Cell viability was determined by measuring the mitochondrial-dependent reduction of MTT (Sigma Aldrich, MO, USA) to formazan [40]. Macrophages in confluence were incubated in the presence of 0.3-10 µM of the compounds for 2 and 24 h in DMEM at 37 ^{o}C and 5% CO_2. Then, the medium was replaced by Dulbecco's PBS containing MTT (0.1 mg mL^{-1}) and the cells were incubated at 37 ºC for 3 h. Formazan crystals were dissolved with DMSO (90:10 v/v) in glycine buffer, containing 0.1 M NaCl, 0.5 mM EDTA, 0.1 M glycine, pH 10.5. The absorbance was measured at 560 nm using the Varioskan Flash plate reader (Thermo, Vantaa, Finland).

Inflammasome activation. Confluent cell monolayers were incubated in 24 well plates in the absence and the presence of 5 µM of the dimethylamine derivatives for 1 h. The cells were activated with 400 U/mL interferon γ (IFN-γ, Sigma) and 8 µg/mL of *Salmonella enterica* LPS (Sigma L7770) for 4 h in DMEM at 37 ^{o}C, 5% CO_2, as described before [21]. Next, the cells were harvested and the proteins from complete cell lysates were resolved in 15% SDS-PAGE, transferred to PVDF membranes and proved with a rabbit polyclonal antibody against IL-1β (Abcam Inc., Cambridge, MA), followed by a donkey anti-rabbit IgG H&L conjugated to Alexa Fluor 680 (Abcam Inc., Cambridge, MA). Blots were scanned using G:BOX, Chemi XT4 (Syngene,

Cambridge, UK), and band intensities analyzed using ImageJ 1.47v (NIH, USA). Paired gels stained with Colloidal blue were run each time to account for protein load (Figure S2)

Statistical analysis. Data are representative or were expressed as mean ± standard deviation from at least three experiments and were analyzed by ANOVA one way considering a significance level of $p < 0.05$.

Acknowledgements

This research was partially supported by Comisión Sectorial de Investigaciones Científicas (CSIC), Universidad de la República and PEDECIBA. LC and BM received doctoral scholarships, from Agencia Nacional de Investigación e Innovación (ANII, Uruguay).

Competing interests

None.

References

[1] J. Holtzman and M. Gross, Lipids, Oxidation, and Cardiovascular Disease, in: Atheroscler. Oxid. Stress, Springer, 2008: pp. 79–95.

[2] T.M. McIntyre, S.L. Hazen, Lipid oxidation and cardiovascular disease: introduction to a review series, Circ. Res. 107 (2010) 1167–1169. doi:10.1161/CIRCRESAHA.110.224618.

[3] J.M. Abais, M. Xia, Y. Zhang, K.M. Boini, P.-L. Li, Redox regulation of NLRP3 inflammasomes: ROS as trigger or effector?, Antioxid. Redox Signal. 22 (2015) 1111–1129. doi:10.1089/ars.2014.5994.

[4] M. Xia, K.M. Boini, J.M. Abais, M. Xu, Y. Zhang, P.-L. Li, Endothelial NLRP3 inflammasome activation and enhanced neointima formation in mice by adipokine visfatin, Am. J. Pathol. 184 (2014) 1617–1628. doi:10.1016/j.ajpath.2014.01.032.

[5] A. Abderrazak, T. Syrovets, D. Couchie, K. El Hadri, B. Friguet, T. Simmet, M. Rouis, NLRP3 inflammasome: From a danger signal sensor to a regulatory node of oxidative stress and inflammatory diseases, Redox Biol. 4 (2015) 296–307. doi:10.1016/j.redox.2015.01.008.

[6] I. Parastatidis, L. Thomson, D.M. Fries, R.E. Moore, J. Tohyama, X. Fu, S.L. Hazen, H.F.G. Heijnen, M.K. Dennehy, D.C. Liebler, D.J. Rader, H. Ischiropoulos, Increased protein nitration burden in the atherosclerotic lesions and plasma of apolipoprotein A-I deficient mice, Circ. Res. 101 (2007) 368–376. doi:10.1161/CIRCRESAHA.107.157537.

[7] L. Thomson, 3-nitrotyrosine modified proteins in atherosclerosis, Dis. Markers. 2015 (2015) 708282. doi:10.1155/2015/708282.

[8] L. Thomson, M. Tenopoulou, R. Lightfoot, E. Tsika, I. Parastatidis, M. Martinez, T.M. Greco, P.-T. Doulias, Y. Wu, W.H.W. Tang, S.L. Hazen, H. Ischiropoulos, Immunoglobulins against tyrosine-nitrated epitopes in coronary artery disease, Circulation. 126 (2012) 2392–2401. doi:10.1161/CIRCULATIONAHA.112.103796.

[9] V.V. Kunjathoor, M. Febbraio, E.A. Podrez, K.J. Moore, L. Andersson, S. Koehn, J.S. Rhee, R. Silverstein, H.F. Hoff, M.W. Freeman, Scavenger Receptors Class A-I/II and CD36 Are the Principal Receptors Responsible for the Uptake of Modified Low Density Lipoprotein Leading to Lipid Loading in Macrophages, J. Biol. Chem. 277 (2002) 49982–49988. doi:10.1074/jbc.M209649200.

[10] D.A. Chistiakov, A.A. Melnichenko, V.A. Myasoedova, A.V. Grechko, A.N. Orekhov, Mechanisms of foam cell formation in atherosclerosis, J. Mol. Med. Berl. Ger. 95 (2017) 1153–1165. doi:10.1007/s00109-017-1575-8.

[11] P. Duewell, H. Kono, K.J. Rayner, C.M. Sirois, G. Vladimer, F.G. Bauernfeind, G.S. Abela, L. Franchi, G. Nuñez, M. Schnurr, T. Espevik, E. Lien, K.A. Fitzgerald, K.L. Rock, K.J. Moore, S.D. Wright, V. Hornung, E. Latz, NLRP3 inflamasomes are required for atherogenesis and activated by cholesterol crystals that form early in disease, Nature. 464 (2010) 1357–1361. doi:10.1038/nature08938.

[12] M. Febbraio, E.A. Podrez, J.D. Smith, D.P. Hajjar, S.L. Hazen, H.F. Hoff, K. Sharma, R.L. Silverstein, Targeted disruption of the class B scavenger receptor CD36 protects against atherosclerotic lesion development in mice, J. Clin. Invest. 105 (2000) 1049–1056. doi:10.1172/JCI9259.

[13] H. Suzuki, Y. Kurihara, M. Takeya, N. Kamada, M. Kataoka, K. Jishage, O. Ueda, H. Sakaguchi, T. Higashi, T. Suzuki, Y. Takashima, Y. Kawabe, O. Cynshi, Y. Wada, M. Honda, H. Kurihara, H. Aburatani, T. Doi, A. Matsumoto, S. Azuma, T. Noda, Y. Toyoda, H. Itakura, Y. Yazaki, S. Horiuchi, K. Takahashi, J.K. Kruijt, T.J.C. van Berkel, U.P. Steinbrecher, S. Ishibashi, N. Maeda, S. Gordon, T. Kodama, A role for macrophage scavenger receptors in atherosclerosis and susceptibility to infection, Nature. 386 (1997) 292. doi:10.1038/386292a0.

[14] T. Karasawa, M. Takahashi, Role of NLRP3 Inflammasomes in Atherosclerosis, J. Atheroscler. Thromb. 24 (2017) 443–451. doi:10.5551/jat.RV17001.

[15] K. Rajamäki, J. Lappalainen, K. Öörni, E. Välimäki, S. Matikainen, P.T. Kovanen, K.K. Eklund, Cholesterol Crystals Activate the NLRP3 Inflammasome in Human Macrophages: A Novel Link between Cholesterol Metabolism and Inflammation, PLOS ONE. 5 (2010) e11765. doi:10.1371/journal.pone.0011765.

[16] X. Li, N. Deroide, Z. Mallat, The role of the inflammasome in cardiovascular diseases, J. Mol. Med. Berl. Ger. 92 (2014) 307–319. doi:10.1007/s00109-014-1144-3.

[17] M. Takahashi, Role of the inflammasome in myocardial infarction, Trends Cardiovasc. Med. 21 (2011) 37–41. doi:10.1016/j.tcm.2012.02.002.

[18] P.L. Thompson, S.M. Nidorf, Anti-inflammatory therapy with canakinumab for atherosclerotic disease: lessons from the CANTOS trial, J. Thorac. Dis. 10 (2018) 695–698. doi:10.21037/jtd.2018.01.119.

[19] P. Welsh, G. Grassia, S. Botha, N. Sattar, P. Maffia, Targeting inflammation to reduce cardiovascular disease risk: a realistic clinical prospect?, Br. J. Pharmacol. 174 (n.d.) 3898–3913. doi:10.1111/bph.13818.

[20] L. Celano, C. Carabio, R. Frache, N. Cataldo, H. Cerecetto, M. González, L. Thomson, Arylnitroalkenes as scavengers of macrophage-generated oxidants, Eur. J. Med. Chem. 74 (2014) 31–40. doi:10.1016/j.ejmech.2013.12.029.

[21] L. Celano, Y.K. Cupertino Da Silva, N. Cataldo, M. Gabay, A. Merlino, M.S. Alexandre-Moreira, L.M. Lima, H. Cerecetto, M. González, L. Thomson, Analgesic and Anti-Inflammatory Properties of Arylnitroalkenes, Inflamm. Allergy Drug Targets. 14 (2015) 19–28.

[22] K.-C. Liang, C.-W. Lee, W.-N. Lin, C.-C. Lin, C.-B. Wu, S.-F. Luo, C.-M. Yang, Interleukin-1β induces MMP-9 expression via p42/p44 MAPK, p38 MAPK, JNK, and nuclear factor-κB signaling pathways in human tracheal smooth muscle cells, J. Cell. Physiol. 211 (2007) 759–770. doi:10.1002/jcp.20992.

[23] M. Boiani, L. Boiani, A. Merlino, P. Hernández, A. Chidichimo, J.J. Cazzulo, H. Cerecetto, M. González, Second generation of 2H-benzimidazole 1,3-dioxide derivatives as anti-trypanosomatid agents: synthesis, biological evaluation, and mode of action studies, Eur. J. Med. Chem. 44 (2009) 4426–4433. doi:10.1016/j.ejmech.2009.06.014.

[24] A. Merlino, M. Boiani, H. Cerecetto, M. González, 2-Benzyl-2-methyl-2H-benzimidazole 1,3-dioxide derivatives: Spectroscopic and theoretical study, Spectrochim. Acta. A. Mol. Biomol. Spectrosc. 67 (2007) 540–549. doi:10.1016/j.saa.2006.08.013.

[25] J. Werber, Y.J. Wang, M. Milligan, X. Li, J.A. Ji, Analysis of 2,2′-azobis (2-amidinopropane) dihydrochloride degradation and hydrolysis in aqueous solutions, J. Pharm. Sci. 100 (2011) 3307–3315. doi:10.1002/jps.22578.

[26] Corwin Hansch, Albert Leo, Substituent constants for correlation analysis in chemistry and biology, Johm Wiley & Sons Inc, New York, 1979.

[27] S. Xu, Y. Huang, Y. Xie, T. Lan, K. Le, J. Chen, S. Chen, S. Gao, X. Xu, X. Shen, H. Huang, P. Liu, Evaluation of foam cell formation in cultured macrophages: an improved method with Oil Red O staining and DiI-oxLDL uptake, Cytotechnology. 62 (2010) 473–481. doi:10.1007/s10616-010-9290-0.
[28] H. Cai, D.G. Harrison, Endothelial dysfunction in cardiovascular diseases: the role of oxidant stress, Circ. Res. 87 (2000) 840–844.
[29] R. Stocker, The ambivalence of vitamin E in atherogenesis, Trends Biochem. Sci. 24 (1999) 219–223.
[30] D. Steinberg, J.L. Witztum, Is the oxidative modification hypothesis relevant to human atherosclerosis? Do the antioxidant trials conducted to date refute the hypothesis?, Circulation. 105 (2002) 2107–2111.
[31] M.A. Moser, O.K. Chun, Vitamin C and Heart Health: A Review Based on Findings from Epidemiologic Studies, Int. J. Mol. Sci. 17 (2016) 1328. doi:10.3390/ijms17081328.
[32] D.P. Vivekananthan, M.S. Penn, S.K. Sapp, A. Hsu, E.J. Topol, Use of antioxidant vitamins for the prevention of cardiovascular disease: meta-analysis of randomised trials, Lancet Lond. Engl. 361 (2003) 2017–2023. doi:10.1016/S0140-6736(03)13637-9.
[33] A. Grebe, F. Hoss, E. Latz, NLRP3 Inflammasome and the IL-1 Pathway in Atherosclerosis, Circ. Res. 122 (2018) 1722–1740. doi:10.1161/CIRCRESAHA.118.311362.
[34] P.M. Ridker, B.M. Everett, T. Thuren, J.G. MacFadyen, W.H. Chang, C. Ballantyne, F. Fonseca, J. Nicolau, W. Koenig, S.D. Anker, J.J.P. Kastelein, J.H. Cornel, P. Pais, D. Pella, J. Genest, R. Cifkova, A. Lorenzatti, T. Forster, Z. Kobalava, L. Vida-Simiti, M. Flather, H. Shimokawa, H. Ogawa, M. Dellborg, P.R.F. Rossi, R.P.T. Troquay, P. Libby, R.J. Glynn, CANTOS Trial Group, Antiinflammatory Therapy with Canakinumab for Atherosclerotic Disease, N. Engl. J. Med. 377 (2017) 1119–1131. doi:10.1056/NEJMoa1707914.
[35] P.M. Ridker, J.G. MacFadyen, B.M. Everett, P. Libby, T. Thuren, R.J. Glynn, CANTOS Trial Group, Relationship of C-reactive protein reduction to cardiovascular event reduction following treatment with canakinumab: a secondary analysis from the CANTOS randomised controlled trial, Lancet Lond. Engl. 391 (2018) 319–328. doi:10.1016/S0140-6736(17)32814-3.
[36] B. Ou, M. Hampsch-Woodill, R.L. Prior, Development and validation of an improved oxygen radical absorbance capacity assay using fluorescein as the fluorescent probe, J. Agric. Food Chem. 49 (2001) 4619–4626.
[37] F. Amen, A. Machin, C. Touriño, I. Rodríguez, A. Denicola, L. Thomson, N-acetylcysteine improves the quality of red blood cells stored for transfusion, Arch. Biochem. Biophys. 621 (2017) 31–37. doi:10.1016/j.abb.2017.02.012.
[38] F. Liu, H. Mizukami, S. Sarnaik, A. Ostafin, Calcium-dependent human erythrocyte cytoskeleton stability analysis through atomic force microscopy, J. Struct. Biol. 150 (2005) 200–210. doi:10.1016/j.jsb.2005.02.001.
[39] T.S. Fisher, P.L. Surdo, S. Pandit, M. Mattu, J.C. Santoro, D. Wisniewski, R.T. Cummings, A. Calzetta, R.M. Cubbon, P.A. Fischer, A. Tarachandani, R.D. Francesco, S.D. Wright, C.P. Sparrow, A. Carfi, A. Sitlani, Effects of pH and Low Density Lipoprotein (LDL) on PCSK9-dependent LDL Receptor Regulation, J. Biol. Chem. 282 (2007) 20502–20512. doi:10.1074/jbc.M701634200.
[40] T. Mosmann, Rapid colorimetric assay for cellular growth and survival: application to proliferation and cytotoxicity assays, J. Immunol. Methods. 65 (1983) 55–63.

Highlights

- Inflammation and oxidative stress have a pivotal role on atherosclerosis
- Arilnitroalkenes, and in particular the dimethylamino derivatives were shown to inhibit both oxidative stress and inflammation
- Moreover, newly synthetized arylnitroalkanes were even more effective than the unsaturated analogous to prevent LDL oxidation and inflammasome activation
- The lead compounds appear as promising multitarget therapies for atherosclerosis due to its antioxidant and anti-inflammatory properties.